Pulmonary Arterial Hypertension Is Linked to Insulin Resistance and Reversed by Peroxisome Proliferator–Activated Receptor-γ Activation

Georg Hansmann, MD; Roger A. Wagner, MD, PhD; Stefan Schellong, BA; Vinicio A. de Jesus Perez, MD; Takashi Urashima, MD; Lingli Wang, MD; Ahmad Y. Sheikh, MD; Renée S. Suen, BSc; Duncan J. Stewart, MD; Marlene Rabinovitch, MD

Background—Patients with pulmonary arterial hypertension (PAH) have reduced expression of apolipoprotein E (apoE) and peroxisome proliferator–activated receptor-γ in lung tissues, and deficiency of both has been linked to insulin resistance. ApoE deficiency leads to enhanced platelet-derived growth factor signaling, which is important in the pathobiology of PAH. We therefore hypothesized that insulin-resistant apoE-deficient ($apoE^{-/-}$) mice would develop PAH that could be reversed by a peroxisome proliferator–activated receptor-γ agonist (eg, rosiglitazone).

Methods and Results—We report that $apoE^{-/-}$ mice on a high-fat diet develop PAH as judged by elevated right ventricular systolic pressure. Compared with females, male $apoE^{-/-}$ were insulin resistant, had lower plasma adiponectin, and had higher right ventricular systolic pressure associated with right ventricular hypertrophy and increased peripheral pulmonary artery muscularization. Because male $apoE^{-/-}$ mice were insulin resistant and had more severe PAH than female $apoE^{-/-}$ mice, we treated them with rosiglitazone for 4 and 10 weeks. This treatment resulted in markedly higher plasma adiponectin, improved insulin sensitivity, and complete regression of PAH, right ventricular hypertrophy, and abnormal pulmonary artery muscularization in male $apoE^{-/-}$ mice. We further show that recombinant apoE and adiponectin suppress platelet-derived growth factor-BB–mediated proliferation of pulmonary artery smooth muscle cells harvested from $apoE^{-/-}$ or C57Bl/6 control mice.

Conclusions—We have shown that insulin resistance, low plasma adiponectin levels, and deficiency of apoE may be risk factors for PAH and that peroxisome proliferator–activated receptor-γ activation can reverse PAH in an animal model. (***Circulation*. 2007;115:1275-1284.**)

Key Words: apolipoproteins ■ glucose ■ hypercholesterolemia ■ hypertension, pulmonary ■ insulin ■ metabolism ■ PPAR gamma

Although insulin resistance is associated with systemic cardiovascular disease,[1–3] it has not been implicated as a predisposing factor in pulmonary arterial hypertension (PAH). Several findings, however, support such an association. Patients with idiopathic PAH have reduced pulmonary mRNA expression of peroxisome proliferator–activated receptor gamma (PPARγ),[4] a ligand-activated nuclear receptor and transcription factor that regulates adipogenesis and glucose metabolism.[5–7] They also have reduced pulmonary mRNA expression of apolipoprotein E (apoE),[8] a protective factor known to reduce circulating oxidized low-density lipoprotein and atherogenesis in the vessel wall.[9] Deficiency of both PPARγ and apoE has been linked to insulin resistance and the metabolic syndrome.[7,9] Elevated levels of several circulating factors that are normally repressed by PPARγ are associated with insulin resistance[3] and implicated in the pathobiology of PAH. These include interleukin-6,[10,11] fractalkine,[12,13] monocyte chemoattractant protein-1,[14] endothelin-1 (ET-1),[15–17] and the endogenous nitric oxide synthase inhibitor asymmetric dimethylarginine (ADMA).[18,19]

Clinical Perspective p 1284

Heightened signaling by platelet-derived growth factor-BB (PDGF-BB)/mitogen-activated protein kinase leading to smooth muscle cell (SMC) proliferation and migration is also a key clinical feature of pulmonary vascular disease.[20–22] With apoE deficiency, abundant oxidized low-density lipoprotein[23] and PDGF-BB[23] were shown to induce mitogen-

Received September 8, 2006; accepted December 29, 2006.

From the Department of Pediatrics, Division of Pediatric Cardiology (G.H., S.S., V.A.D.J.P., T.U., L.W., M.R.), Department of Medicine, Division of Cardiovascular Medicine (R.A.W.), and Department of Cardiovascular Surgery (A.Y.S.), Stanford University School of Medicine, Stanford, Calif, and Department of Medicine, Division of Cardiology, University of Toronto, Toronto, Ontario, Canada (R.S.S., D.J.S.).

The online-only Data Supplement, consisting of expanded Methods and tables, is available with this article at http://circ.ahajournals.org/cgi/content/full/CIRCULATIONAHA.106.663120/DC1.

Correspondence to Dr Marlene Rabinovitch, Vera Moulton Wall Center for Pulmonary Vascular Disease, Stanford University School of Medicine, CCSR 2245B, 269 Campus Dr, Stanford, CA 94305-5162. E-mail marlener@stanford.edu

Circulation **is available at http://www.circulationaha.org** **DOI: 10.1161/CIRCULATIONAHA.106.663120**

activated protein kinase, transcription of growth-promoting genes (eg, cyclin D1), and subsequently proliferation and migration of systemic vascular SMCs.[23,24] Interestingly, high glucose concentrations induce mitogen-activated protein kinase/phosphatidylinositol 3-kinase (PI3K)–dependent up-regulation of PDGF receptor-β (PDGFR-β) and potentiate SMC migration in response to PDGF-BB.[24] In concert with PI3K, PDGFR-β/mitogen-activated protein kinase-signaling also leads to SMC resistance to apoptosis.[25]

In systemic vascular SMCs, apoE and adiponectin,[26] a PPARγ target in adipocytes,[7] inhibit PDGF-BB–induced SMC proliferation and migration.[23,27] ApoE internalizes the PDGFR-β,[28–30] and adiponectin sequesters the ligand PDGF-BB.[31] Thus, in association with insulin resistance, reduced levels of apoE[23] and adiponectin[27] can be expected to enhance PDGF-BB signaling. In accordance with these observations, diabetic apoE-deficient (apoE$^{-/-}$) mice show pronounced PDGF-BB signaling and neointimal thickening of the arterial vessel wall.[32] We hypothesized that these factors would have similar effects on pulmonary arterial SMCs (PASMCs), consequently leading to PAH.

PPARγ agonists are clinically used to make cells insulin sensitive, thereby obviating the detrimental effects of insulin resistance related to hyperlipidemia, inflammation, and mitogenesis in the vessel wall.[33] Rosiglitazone, a PPARγ ligand of the thiazolidinedione class, enhances insulin-mediated glucose uptake and inhibits proliferation and migration of systemic SMCs induced by PDGF-BB.[33,34] We therefore hypothesized that PAH would develop in apoE$^{-/-}$ insulin-resistant mice but that the disease process would be attenuated or reversed by a PPARγ agonist (eg, rosiglitazone).

In the present study, we show that apoE deficiency, in association with a high-fat (HF) diet, leads to both insulin resistance and PAH. Male apoE$^{-/-}$ mice had more severe PAH (ie, higher right ventricular systolic pressure [RVSP], right ventricular hypertrophy [RVH], and enhanced peripheral PA muscularization) associated with insulin resistance and lower plasma adiponectin levels compared with female apoE$^{-/-}$ mice. Because testosterone inhibits the secretion of adiponectin in adipocytes,[35] we hypothesized that elevation of this vasoprotective adipocytokine may account for the less severe vascular phenotype in female apoE$^{-/-}$ mice. We therefore treated male apoE$^{-/-}$ mice with rosiglitazone and documented 8-fold-higher plasma adiponectin levels, improved insulin sensitivity, and complete regression of PAH, RVH, and abnormal PA muscularization. To further establish a direct link between apoE and adiponectin and SMC proliferation and survival, we treated murine (apoE$^{-/-}$ and wild-type) PASMCs in culture with recombinant apoE and adiponectin. We showed that both proteins inhibit PDGF-BB–induced proliferation in apoE$^{-/-}$ and wild-type PASMCs. Our data therefore suggest that insulin resistance and deficiency of apoE and/or adiponectin may be risk factors for PAH that can be reversed by PPARγ activation.

Methods

Expanded Methods and Results sections are given in the online Data Supplement.

Experimental Design

ApoE$^{-/-}$ mice (B6.129P2-Apoetm1Unc/J) and C57Bl/6 control mice were obtained from Jackson Laboratories (Bar Harbor, Me). At 4 weeks of age, the mice were either continued on regular chow or switched to HF diet (Dyets No. 101511, Dyets Inc, Bethlehem, Pa) for a maximum of 21 weeks. For the nontreatment study, 15-week-old male and female mice (apoE$^{-/-}$, C57Bl/6 controls) on either diet were studied. For the rosiglitazone treatment study, 15-week-old male mice (apoE$^{-/-}$, C57Bl/6 controls) on HF diet were used. Half of the animals received rosiglitazone (GlaxoSmithKline, Research Triangle Park, NC) 10 mg/kg body weight per day PO incorporated into the food for 4 or 10 weeks. All protocols were approved by the Stanford Animal Care Committee.

Hemodynamic Measurements

Measurements of RVSP and RV dP/dt were performed by jugular vein catheterization (1.4F, Millar Instruments Inc, Houston, Tex) under isoflurane anesthesia (1.5% to 2.5%) using a closed-chest technique in unventilated mice at 15, 19, and 25 weeks of age. Left ventricular (LV) end-diastolic pressure was determined by LV catheterization via the left carotid artery under isoflurane anesthesia. Systemic blood pressure was determined by the tail-cuff method in nonanesthesized mice. Measurements of cardiac output and function were performed by echocardiography.

RVH and LV Hypertrophy

RVH was measured by the weight of the RV relative to LV+septum. LV hypertrophy was measured as absolute weight of the LV plus septum. LV dilatation was assessed by echocardiographic M-mode measurement of the LV end-diastolic inner diameter.

Lung Tissue Preparation

Lungs were perfused with normal saline, fixed in 10% formalin overnight, and then either embedded in paraffin for standard histology or frozen for Oil-red-O staining. A subset of left lungs (approximately half) were barium infused via PA-inserted tubing to label peripheral PAs for morphometric analysis and micro–computed tomography (CT) imaging.

Morphometric Analysis

Transverse left lung sections were stained by elastic van Gieson and Movat pentachrome stains. From all mice, we took the same full section in the mid portion of the lung parallel to the hilum and embedded it in the same manner. Muscularization was assessed in barium-injected left lung sections by calculating the proportion of fully and partially muscularized peripheral (alveolar wall) PAs to total peripheral PAs. All measurements were done blinded to genotype and condition.

Micro-CT Imaging

A custom-built eXplore Locus RS120 Micro CT Scanner (GE Health Care, Ontario, Canada) was used to acquire nondestructing 3-dimensional images of barium-infused whole-lung specimens. Images were scanned at 49-μm resolution and 720 views (70 kV [peak], 50 mAmps, 30-ms single image acquisition time) and reconstructed with the eXplore Reconstruction Utility, and volumes were viewed and rendered with the GE Health Care MicroView software.

Fasting Whole-Blood and Plasma Measurements

We performed tail vein puncture in nonanesthetized, overnight-starved mice, followed by duplicate whole-blood glucose measurements with a glucometer (Freestyle/Abbott). Fasting blood plasma was obtained via retro-orbital bleeding or cardiac puncture. White blood cell count and hematocrit were assessed by the Stanford Animal Facility Laboratories. Hemoglobin A1c was measured by Esoterix (Calabasa Hills, Calif). Plasma ET-1 was measured by ELISA. Plasma ADMA levels were determined by high-performance liquid tomography at Oxonon Bioanalysis Inc (Oakland, Calif). All

other plasma measurements were done in duplicate at Linco Diagnostics (St Charles, Mo).

Cell Culture

Primary murine PASMCs were isolated from apoE$^{-/-}$ and C57Bl/6 mice using a modified elastase/collagenase digestion protocol as previously described.[36] Murine PASMCs were grown to 70% confluence and cultured in starvation media (DMEM, 0.1% FBS, 100 U/mL penicillin, 0.1 mg/mL streptomycin) for 24 hours. Recombinant apoE (Chemicon International, Temecula, Calif) and adiponectin (BioVision, Mountain View, Calif) were added to quiescent cells 30 minutes before mitogenic stimulation with PDGF-BB (R&D Systems, Minneapolis, Minn).

Cell Proliferation Assays

For cell counts, PASMCs were seeded at 2.5×10^4 cells per well of a 24-well plate in growth medium and allowed to adhere overnight. The medium was removed, and the cells were washed 3 times with PBS and incubated in starvation media for 24 hours, followed by PDGF-BB stimulation (20 ng/mL) for 0 and 72 hours. Cells were then washed with PBS, trypsinized, resuspended, and counted in a hemacytometer.

Statistical Analysis

Values from multiple experiments are expressed as mean±SEM. Using the Kohmogorov-Smirnov test and larger data sets from previous studies, we could show that the measured values were approximately normally distributed. Statistical significance was determined using 1-way ANOVA, followed by Bonferroni's multiple-comparison test unless stated otherwise. A value of $P<0.05$ was considered significant. The significance of our data also was confirmed by the nonparametric Mann-Whitney test. The number in each group is indicated in the column graphs and in the figure legends. For some of the metabolic measurements such as blood glucose, which did not require invasive blood draws, a larger number of animals could be assessed, resulting in minor unevenness in the numbers reported.

All authors had full access to and take full responsibility for the integrity of the data. All authors have read and agree to the manuscript as written.

Results

ApoE$^{-/-}$ and C57Bl/6 Mice on Regular Chow Have Similar RVSPs and RV Mass

First, we assessed 15-week-old male and female apoE$^{-/-}$ mice on regular chow for the presence and severity of PAH. Values of RVSP, a measure of PAH, and of RV/LV+septum ratio, a measure of RVH, were similar in apoE$^{-/-}$ and C57Bl/6 control mice. Moreover, no significant differences were observed in RVSP or RV/LV+septum ratio between genders of either genotype (Table 1).

ApoE$^{-/-}$ Mice on HF Diet Develop PAH

An 11-week HF diet treatment did not significantly increase RVSP in 15-week old C57Bl/6 mice (Table 1). In contrast, apoE$^{-/-}$ mice on HF diet for the same duration developed PAH as judged by significant elevation in RVSP, with males having higher values than females (Figure 1A and Table 1). In addition, only male apoE$^{-/-}$ mice on HF diet had RVH and enhanced peripheral PA muscularization (Figure 1B and 1C) compared with C57Bl/6 controls ($P<0.001$). A direct comparison revealed a more severe PAH phenotype in the male versus female apoE$^{-/-}$ mice on HF diet in that RVSP (28.9 versus 24.9 mm Hg; $P=0.0014$), RVH (RV/LV+septum ratio, 0.41 versus 0.29; $P=0.0093$), and peripheral muscularization (47.8 versus 35.4%; $P=0.0371$) were significantly greater (Figure 1A through 1C, unpaired 2-tailed t test). RV systolic function (RV dP/dtmax) was augmented in apoE$^{-/-}$ mice of both genders and reflected the elevated RVSP compared with C57Bl/6 controls (Table 1). RV diastolic function (RV dP/dtmin) was greater in both male (trend) and female ($P<0.05$) apoE$^{-/-}$ mice compared with C57Bl/6 mice of the same gender. Systemic blood pressure, cardiac output, LV function (indicated by LV end-diastolic pressure of 2 to 5 mm Hg), and hematocrit were similar in both genotypes (Table 1). Thus, the elevation of RVSP in apoE$^{-/-}$ compared with C57Bl/6 mice likely reflected an elevation in pulmonary vascular resistance.

PA Atherosclerosis in the ApoE$^{-/-}$ Mice Does Not Cause Significant PA Stenosis

Further studies were carried out to determine whether apoE$^{-/-}$ mice on HF diet developed, in addition to neomuscularization of peripheral PAs, occlusive atheroma accounting for the elevated RVSP and RVH compared with C57Bl/6 mice. Micro-CT imaging of barium-injected lungs revealed an irregularly shaped main PA vessel wall in male and female apoE$^{-/-}$ mice on HF diet but excluded PA branch stenosis as contributing to the RVSP elevation (Figure 1F and 1G). This feature was associated with nonocclusive atherosclerotic lesions only in large intrapulmonary arteries (diameter ≥500 μm) in apoE$^{-/-}$ mice of both genders on HF diet (see Figure I in the online Data Supplement). Atherosclerotic lesions were neither seen in C57Bl/6 control mice on HF diet nor in mice of both genotypes on regular chow.

Insulin Resistance Is Associated With More Severe PAH in Male ApoE$^{-/-}$ Mice

We focused our attention on possible differences in the lipid profile and markers of insulin resistance associated with the more severe PAH phenotype in apoE$^{-/-}$ versus C57Bl/6 mice, particularly in male versus female apoE$^{-/-}$ mice. Higher plasma cholesterol (mainly non–high-density lipoprotein cholesterol) was observed in male and female apoE$^{-/-}$ mice compared with C57Bl/6 controls on HF diet. In addition, apoE$^{-/-}$ mice had moderately higher triglyceride levels that were similar in male and female apoE$^{-/-}$ mice and independent of the diet (Tables I and II in the online Data Supplement). However, only in male apoE$^{-/-}$ and not female apoE$^{-/-}$ mice on HF diet did we observe features consistent with insulin resistance (ie, elevated fasting blood glucose and insulin levels), compared with C57Bl/6 controls (Figure 2).

Because of the concordance of insulin resistance and the more severe PAH phenotype in male versus female apoE$^{-/-}$ mice, we investigated whether the females had higher plasma levels of the insulin-sensitizing adipocytokines adiponectin and leptin. Although the HF diet resulted in a marked increase in adiponectin and leptin levels in control C57Bl/6 mice of both genders, this marked upregulation was absent in apoE$^{-/-}$ mice (for adiponectin, see Figure 2A and 2B; for leptin, see Tables I and II in the online Data Supplement). It is therefore possible that the release of adiponectin and leptin from adipocytes in response to HF diet is to some extent apoE dependent. However, female mice of both genotypes had

TABLE 1. RVSP and Heart Weight Measurements in C57Bl/6 (Control) and ApoE$^{-/-}$ Mice on Regular Chow and Hemodynamic, Echocardiographic, and Heart Weight Measurements in C57Bl/6 (Control) and ApoE$^{-/-}$ Mice on HF Diet

	Control Males	ApoE$^{-/-}$ Males	Control Females	ApoE$^{-/-}$ Females	*P*	n
Mice on regular chow						
RVSP, mm Hg	20.6±0.8	23.2±0.6	19.7±1.5	22.5±0.8		4–5
RV, mg	26.5±1.3‡	24.9±1.4†	17.9±0.9	18.1±0.7	CM vs CF,‡ AM vs AF†	4–5
RV/LV+S	0.26±0.01	0.30±0.01	0.26±0.01	0.27±0.02		4–5
LV+S, mg	101.0±2.7‡	84.6±4.3*	69.2±2.7	68.6±2.2	CM vs AM,* CM vs CF,‡ AM vs AF*	4–5
Mice on HF diet						
Hemodynamics						
RVSP, mm Hg	20.6±0.5	28.9±0.6‡	20.5±0.9	24.9±0.6†	AM vs CM,‡ AM vs AF,† AF vs CF†	4–5
RV dP/dtmax, mm Hg/s	1132±82	1754±62*	950±206	1513±125*	AM vs CM,* AF vs CF*	4–5
RV dP/dtmin, mm Hg/s	−951±86	−1396±72	−753±173	−1279±96*	AF vs CF*	4–5
Systolic BP, mm Hg	92±1.9	99±2.6	83±5.4	96±1.3		4–5
MAP, mm Hg	79±1.4	85±2.9	77±3.5	86±1.5		4–5
Diastolic BP, mm Hg	73±1.6	77±4.4	71±3.4	80±1.8		4–5
LVEDP, mm Hg	2.4±0.5	2.8±0.2	2.5±0.3	2.7±1.2		4–5
Echocardiography						4–5
Heart rate, bpm	398±29.6	370±22.5	447±27	408±36		4–5
EF, %	74±0.7	77.6±5.4	70.2±2.4	85.7±2.6*	AF vs CF*	4–5
FS, %	37.5±0.6	42.0±6.2	34.3±1.9	51.2±2.9†	AF vs CF†	4–5
CO, mL/min)	30.0±2.1	29.1±5.5	24.3±2.2	24.7±3.8		4–5
LVIDD, mm	3.4±0.06	3.4±0.28	3.1±0.02	3.0±0.13		4–5
LVISD, mm	2.1±0.02	2.0±0.33	2.0±0.06	1.5±0.16		4–5
Heart weight						
RV, mg	19.5±1.3	33.0±4.0†	18.1±0.5	18.0±1.1	AM vs CM,† AM vs AF†	4
RV/LV+S	0.25±0.02	0.41±0.03‡	0.24±0.01	0.29±0.01	AM vs CM,‡ AM vs AF†	4
LV+S, mg	79.3±0.3	81.3±8.3*	74.8±1.4	60.9±2.0	AM vs AF*	4
Blood						
HCT, %	47.1±0.8	44.5±0.9	42.4±2.6	44.8±0.8		4–5
WBC, 10^3 cells/μL	2.1±0.5	1.4±0.4	2.3±0.6	1.2±0.2		4–5

Fifteen-week-old male and female mice on regular chow or HF diet for 11 weeks in normoxia. Statistically significant differences between C57Bl/6 (control) and apoE$^{-/-}$ mice of either gender and between genders of the same genotype are indicated. Values are mean±SEM. CM indicates control males; AM, apoE$^{-/-}$ males; CF, control females; AF, apoE$^{-/-}$ females; S, septum; BP, blood pressure; MAP, mean arterial pressure; LVEDP, LV end-diastolic pressure (determined by left carotid artery/LV catheterization); EF, ejection fraction; FS, fractional shortening; CO, cardiac output; LVIDD, LV end-diastolic inner diameter; LVISD, LV end-systolic inner diameter; HCT, hematocrit; and WBC, white blood cell count.

*$P<0.05$; †$P<0.01$; ‡$P<0.001$.

~50% higher plasma adiponectin levels than their male counterparts (Figure 2A and 2B). Gender differences in leptin levels were difficult to ascertain because of considerable variability in the individual values (Tables I and II in the online Data Supplement). Because testosterone inhibits the secretion of adiponectin in adipocytes,[35] we hypothesized that higher adiponectin levels, in association with lack of insulin resistance, may account for the less severe pulmonary vascular phenotype in female apoE$^{-/-}$ mice on a HF diet.

PPARγ Activation Elevates Plasma Adiponectin, Improves Insulin Sensitivity, and Reverses PAH

On the basis of these data, we reasoned that the presence of PAH may be determined by the inability to sufficiently raise adiponectin levels in association with a HF diet (Figure 2A and 2B) and that the severity of the disease may be a function of the degree of hyperinsulinemia and hyperglycemia (Figure 2C through 2F). We therefore hypothesized that treating the pulmonary hypertensive, insulin-resistant male apoE$^{-/-}$ mice with a PPARγ agonist to increase plasma adiponectin and improve insulin sensitivity might arrest disease progression or reverse PAH. Thus, we treated 15-week-old male apoE$^{-/-}$ and C57Bl/6 control mice on a HF diet with rosiglitazone 10 mg $\cdot$ kg^{-1} $\cdot$ d^{-1} incorporated into their food. The effects of both 4- and 10-week treatments on RVSP, RVH, and metabolic features were assessed. Four-week treatment with rosiglitazone resulted in much higher plasma adiponectin levels in C57Bl/6 control (5-fold) and apoE$^{-/-}$ (8-fold) mice compared with untreated animals of the same genotype (Figure 3A). The higher plasma adiponectin in treated versus untreated apoE$^{-/-}$ mice was associated with lower blood glucose (control level), indicating improved insulin sensitivity in apoE$^{-/-}$ mice treated with rosiglitazone (Figure 3A, 3C, and 3E).

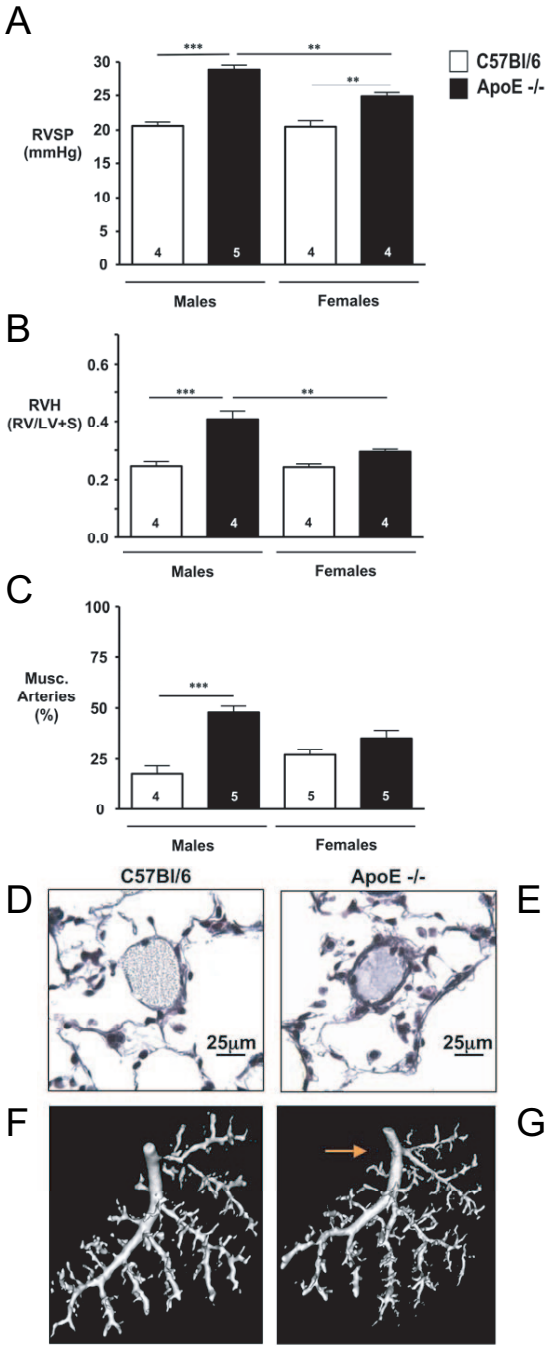

Figure 1. Pulmonary hypertension in apoE$^{-/-}$ mice on HF diet in normoxia. Fifteen-week-old male mice on HF diet for 11 weeks. A, RVSP. B, RVH, measured as ratio of the weight of the right ventricle (RV) to that of left ventricle (LV) plus septum (S). C, Muscularization of alveolar wall arteries. Bars represent mean±SEM (n=4–5 as indicated in column graphs). *P<0.05; **P<0.01; and ***P<0.001. D and E, Representative photomicrographs of lung tissue (stained by Movat pentachrome) of 15-week-old male mice on HF diet showing a typical nonmuscular peripheral alveolar artery in a C57B1/6 mouse (D). A similar section in the apoE$^{-/-}$ mouse shows an alveolar wall artery surrounded by a rim of muscle (E). F and G, Micro-CT imaging of barium-injected pulmonary arteries (PA). Representative irregularly shaped main PA wall is observed in apoE$^{-/-}$ mouse on HF diet (arrow), but significant PA stenoses are excluded in C57B1/6 control (F) and apoE$^{-/-}$ mice (G).

RVSP in untreated C57Bl/6 and apoE$^{-/-}$ mice over this period of time was not significantly different from the baseline values observed in the 15-week-old mice of the initial study (see Figure 1A compared with Figure 3B and Table 1 versus Table 2). In addition to the induction of plasma adiponectin and improvement of insulin sensitivity, a 4-week course of rosiglitazone treatment resulted in lower RVSP, RV mass (RV/LV+septum ratio), and percentage of muscularized arteries at the alveolar wall level that were similar to those in C57Bl/6 control mice (Figure 3B, 3D, and 3F). Because we started treatment at a time when the insulin-resistant male apoE$^{-/-}$ mice already had elevated RVSP, RVH, and peripheral PA muscularization, our findings indicate that we had induced regression of PAH. Rosiglitazone given for 4 weeks caused no significant differences in systemic blood pressure, heart rate, LV systolic function (fractional shortening, ejection fraction), cardiac output, and RV systolic and diastolic function (Table 2). Other measurements such as hematocrit and white blood cell count also were similar in treated and untreated animals. There was, however, a tendency for rosiglitazone to cause mild LV dilatation and increased LV mass in both C57Bl/6 control and apoE$^{-/-}$ mice (Table 2).

All the features described above were sustained after a 10-week rosiglitazone treatment period, suggesting that the effect was not transient. However, at this time point, hematocrit was slightly lower in both control and apoE$^{-/-}$ mice treated with rosiglitazone (Table III in the online Data Supplement). Decreased hematocrit and a tendency for LV dilatation and increased LV mass have been previously reported in the clinical setting as minor side effects of rosiglitazone treatment.[37]

Rosiglitazone Does Not Regulate Plasma ET-1 and ADMA in ApoE$^{-/-}$ Mice

ET-1 and ADMA were measured in blood plasma after a 4-week treatment with rosiglitazone. Plasma ET-1 levels were lower in treated than in untreated C57Bl/6 mice. However, ET-1 levels were lower in apoE$^{-/-}$ compared with C57Bl/6 mice and were not affected by rosiglitazone. ADMA levels were in the normal murine range, not different between genotypes, and not altered by rosiglitazone treatment (Table 2).

Recombinant ApoE and Adiponectin Inhibit PASMC Proliferation

To support possible roles of apoE and adiponectin in protecting against the development of PAH, we showed that both proteins inhibit PDGF-BB–induced proliferation of PASMCs harvested from both C57Bl/6 control and apoE$^{-/-}$ mice (Figure 4A and 4B).

Discussion

Although a link between insulin resistance and systemic cardiovascular disease is evident in both clinical[2] and experimental studies,[3,33] this report is the first indication that there may be a possible link with PAH. If insulin resistance does contribute to the pathobiology of PAH in humans, it will be an extremely important relationship owing to the steadily increasing number of children, adolescents,[1] and adults[2] with

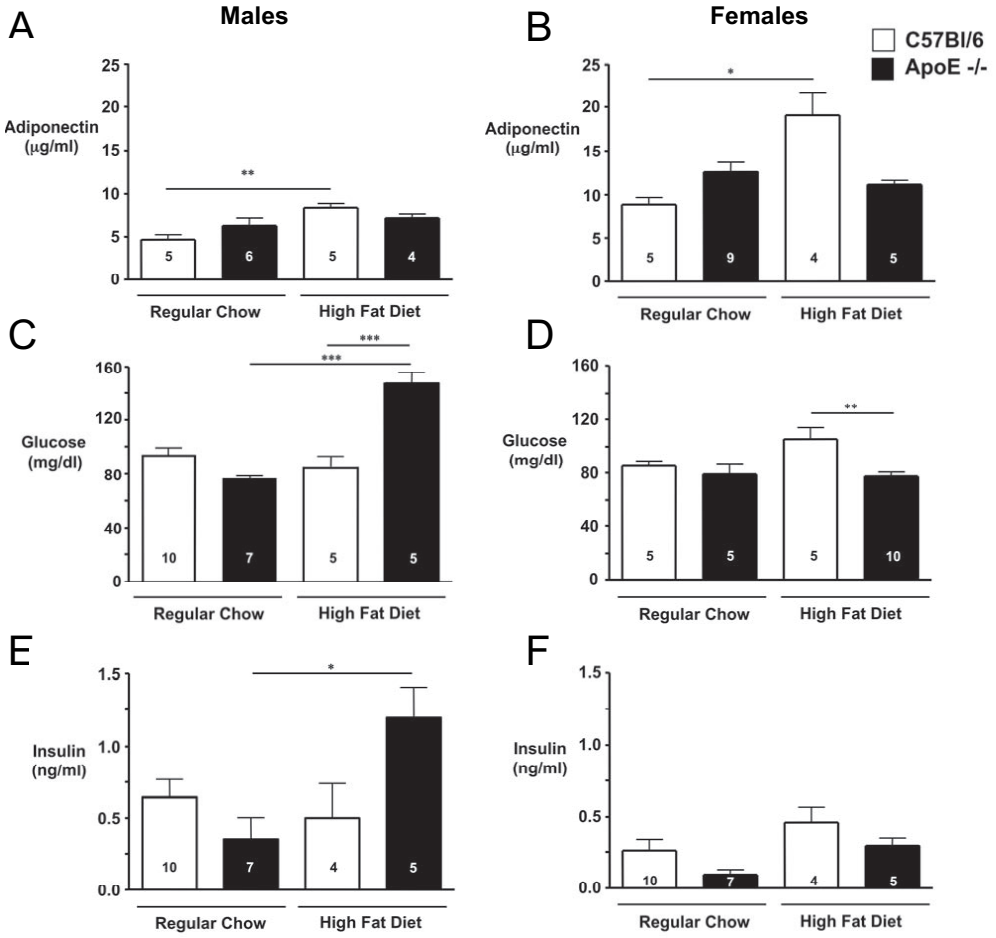

Figure 2. Male but not female apoE$^{-/-}$ mice develop insulin resistance and hypoadiponectinemia on HF diet. Plasma adiponectin (A,B), blood glucose (C, D), and plasma insulin (E, F). Overnight-starved 15-week-old male (A, C, E) and female (B, D, F) C57Bl/6 and apoE$^{-/-}$ mice, on regular chow or HF diet for 11 weeks. Note that C57Bl/6 mice but not apoE$^{-/-}$ mice of both genders upregulate their adiponectin levels when exposed to HF diet. Bars represent mean±SEM (n=5–10 as indicated in column graphs). *$P<0.05$; **$P<0.01$; and ***$P<0.001$.

the metabolic syndrome, which includes insulin resistance as a key element.

ApoE$^{-/-}$ mice of both genders on HF showed atheroma on histology and on micro-CT, affecting the large PAs in a nonocclusive manner. Similar features have been described in pathological specimens of adult patients with PAH.[38] However, the cholesterol levels and the presence of atheroma were similar in male and female apoE$^{-/-}$ mice, but only male apoE$^{-/-}$ developed insulin resistance and severe PAH (ie, a combination of marked RVSP elevation, RVH, and enhanced peripheral PA muscularization). We therefore suggest that apoE deficiency, hypoadiponectinemia, and the related insulin resistance, rather than pulmonary atherosclerosis itself, were the major causes of PAH.

The level of PAH seen in our model, with an RVSP baseline elevation of 7 to 9 mm Hg over controls for males on a HF diet in normoxia, was not based on LV dysfunction and is comparable to[39] or even greater than[40,41] that in the relatively few murine models of PAH described to date. The sole exception is the inducible vascular SMC dominant-negative bone-morphogenetic protein receptor II (BMP-RII) transgenic mouse. However, values in the control mice of this BMP-RII model also were quite elevated, consistent with the relative "hypoxia" at Denver altitude.[42]

The likely mechanism by which apoE deficiency leads to the development of PAH appears to be facilitated by PDGF-BB signaling. From studies in systemic vascular SMCs, we know that PDGF-BB signaling in SMCs is suppressed when apoE binds to the low-density lipoprotein receptor–related protein (LRP), thereby initiating endocytosis and degradation of the LRP–PDGFR-β–PDGF-BB complex.[28–30] We have shown here that PDGF-BB–induced proliferation also is suppressed by apoE in PASMCs, suggesting that a similar mechanism may be present in the pulmonary vasculature. In diabetic apoE$^{-/-}$ mice, PDGFR-β signaling is increased in vascular SMCs, and systemic vascular disease can be reversed by the PDGFR tyrosine kinase inhibitor imatinib.[32] We[40] and others[21] have shown that blockade of tyrosine kinase activity selective to the epidermal growth factor receptor[40] or the PDGFR[21] reverses experimental PAH and vascular remodeling caused by the toxin monocrotaline in rats.

In association with insulin resistance, the male mice (apoE$^{-/-}$ and C57Bl/6) had lower levels of adiponectin than

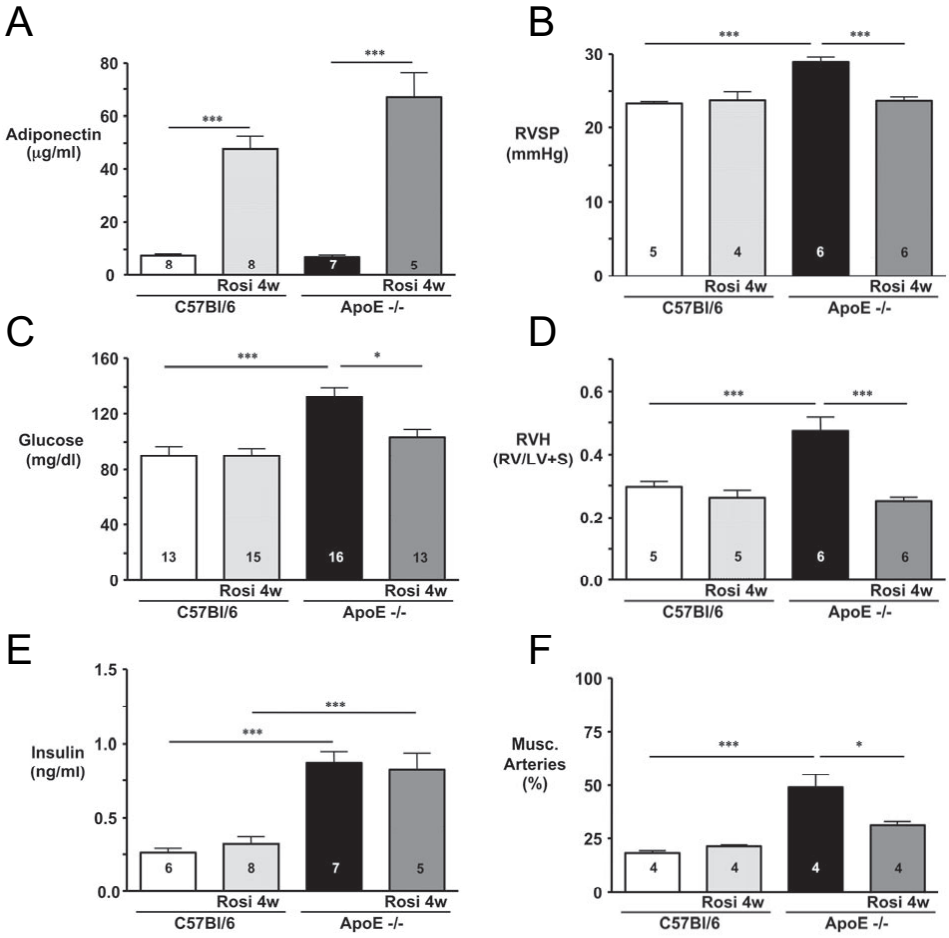

Figure 3. Four-week treatment with the PPARγ agonist rosiglitazone reverses PAH, increases plasma adiponectin, and induces insulin sensitivity. Measurements of plasma adiponectin (A), blood glucose (C) and plasma insulin (E), RVSP (B), RVH (D), and muscularization of alveolar wall arteries (F). Nineteen-week-old male C57Bl/6 and apoE$^{-/-}$ mice, all on HF diet for 15 weeks, were used. Bars represent mean±SEM (n=4–16 as indicated in column graphs). *$P<0.05$; **$P<0.01$; and ***$P<0.001$.

the female mice. This finding is in keeping with a recent study demonstrating that testosterone inhibits the secretion of adiponectin in adipocytes.[35] Adiponectin reverses insulin resistance[26] and is independently associated with a reduced risk of type 2 diabetes mellitus in apparently healthy individuals.[43] Moreover, the high-molecular-weight form of adiponectin binds PDGF-BB, thereby reducing PDGF-BB bioavailability[31] and mitogenic postreceptor function in vascular SMCs.[27] Adiponectin has been shown to be a transcriptional target of PPARγ in adipocytes.[7] Because previous studies used the PPARγ agonist rosiglitazone to suppress intimal thickening in the apoE$^{-/-}$ mouse,[44] we reasoned that it might also be effective in preventing disease progression or reversing PAH. Indeed, treatment of male apoE$^{-/-}$ mice with rosiglitazone increased plasma adiponectin, improved insulin sensitivity, and led to sustained regression of PAH, RVH, and abnormal muscularization of distal PAs. The source of adiponectin in our animal model is likely from visceral and subcutaneous as well as perivascular adipocytes.[17] To further support a mechanistic relationship between apoE and adiponectin deficiency on the one hand and PAH with enhanced muscularization of peripheral arteries on the other, we showed that both recombinant apoE and adiponectin inhibited PDGF-BB–induced proliferation of cultured murine wild-type and apoE$^{-/-}$ PASMCs.

In addition to elevating adiponectin levels and thus causing sequestration of PDGF-BB, PPARγ activation blocks PDGF gene expression[45] and PDGF-BB–mediated systemic SMC proliferation and migration.[33,34] This is likely to occur via inhibition of phosphorylated extracellular-regulated kinase nuclear translocation[46] and/or induction of protein phosphatases[47] that reduce phosphorylated extracellular-regulated kinase. Furthermore, PPARγ induces expression of LRP,[48] the receptor necessary for apoE-mediated suppression of PDGF-BB signaling.[28–30] By blocking important survival pathways downstream of activated PDGFR-β (eg, PI3K),[25] rosiglitazone could also induce apoptosis of proliferating vascular cells.[33,49]

We considered the possibility that PPARγ activation might impair the expression of ET-1[15] and the endogenous nitric oxide synthase inhibitor ADMA,[18] both of which have previously been linked to clinical PAH[16,19] and insulin resistance.[17,18] However, although it is not surprising that rosiglitazone decreased ET-1 levels in the C57Bl/6 mice, we expected the apoE$^{-/-}$ mice to have higher levels of ET-1 under control conditions. In the present study, however, we

TABLE 2. Hemodynamic, Echocardiographic, Heart Weight, Hematocrit, and Other Blood Measurements in Male C57Bl/6 (Control) and ApoE$^{-/-}$ Mice After Treatment With Rosiglitazone for 4 Weeks

Parameter	Control	Control Rosi	ApoE$^{-/-}$	ApoE$^{-/-}$ Rosi	*P*	n
Hemodynamics						
RVSP, mm Hg	23.3±0.2	23.8±1.2	28.9±0.6‡	23.7±0.5‡	A vs C,‡ AR vs A‡	4–6
RV dP/dtmax, mm Hg/s	1543±59	1762±170	1489±154	1668±155		4–6
RV dP/dtmin, mm Hg/s	−1207±104	−1575±198	−1665±147	−1569±128		4–6
Systolic BP, mm Hg	103±3.4	95±2.4	108±4.0	100±2.3		7–8
MAP, mm Hg	85±3.3	78±2.6	90±4.2	80.6±3.2		7–8
Diastolic BP, mm Hg	75±3.3	70±2.8	81±4.4	71±3.9		7–8
Echocardiography						
Heart rate, bpm	369±15.9	356±24.8	295±10.5*	334±16.6	A vs C*	5–7
EF, %	70.0±1.3	70.1±2.3	69.8±1.0	64.4±1.1		5–7
FS, %	34.2±1.0	34.5±1.8	34.1±0.7	30.2±0.8		5–7
CO, mL/min	39.0±3.2	48.7±4.6	32.0±2.6	40.8±2.5		5–7
LVIDD, mm	3.91±0.07	4.27±0.08*	3.97±0.11	4.20±0.06	CR vs C*	5–7
LVISD, mm	2.59±0.04	2.80±0.11	2.63±0.10	2.96±0.07		5–7
LVPWd, mm	0.60±0.03	0.75±0.08	0.72±0.05	0.64±0.06		5–7
IVSd, mm	0.61±0.05	0.58±0.04	0.70±0.06	0.62±0.04		5–7
Heart weight						
RV, mg	27.2±1.2	30.8±3.7	39.5±5.6	26.2±1.7		5–6
RV/LV+S	0.30±0.02	0.26±0.02	0.47±0.04†	0.25±0.01‡	A vs C,† AR vs A‡	5–6
LV+S, mg	92.2±1.4	116.8±6.2*	82.5±6.4	103.5±3.7*	CR vs C,* AR vs A*	5–6
Blood						
HCT, %	45.7±3.5	41.1±2.5	49.7±1.3	51.2±1.5*	AR vs CR*	5–7
WBC, $10^3/\mu$L	5.5±2.2	3.8±1.2	2.0±0.4	3.6±1.0		5–7
ET-1, fmol/L	35.8±5.5	12.5±1.9	11.5±0.9*	14.5±1.4*	A vs C,* CR vs C*	3–5
ADMA, μmol/L	0.24±0.02	0.29±0.05	0.22±0.02	0.21±0.02		4–7

Nineteen-week-old male mice on HF diet for 15 weeks, untreated or treated with rosiglitazone for 4 weeks, in normoxia. Statistically significant differences between C57Bl/6 (control) and apoE$^{-/-}$ mice of either group and between treated and untreated mice of the same genotype are indicated. ET-1 and ADMA were measured in blood plasma. Systemic blood pressure was measured at 24 weeks of age (ie, after treatment with rosiglitazone for 9 weeks). Values are mean±SEM. C indicates control; CR, control treated with rosiglitazone (Rosi); A, ApoE$^{-/-}$; AR, ApoE$^{-/-}$ treated with rosiglitazone; BP, blood pressure; MAP, mean arterial pressure; EF, ejection fraction; FS, fractional shortening; CO, cardiac output; LVIDD, LV end-diastolic inner diameter; LVISD, LV end-systolic inner diameter; LVPWd, LV end-diastolic posterior wall thickness; IVSd, end-diastolic interventricular septum thickness; S, septum; HCT, hematocrit; and WBC, white blood cell count.

*$P<0.05$; †$P<0.01$; ‡$P<0.001$.

could not relate the reversal of PAH with rosiglitazone to a decrease in either ET-1 or ADMA plasma level.

Recently, we made the interesting observation that BMP-2 induces nuclear shuttling and DNA binding of PPARγ in human PASMCs.[50] Loss-of-function mutations in the BMP-RII gene frequently occur in cases of familial and idiopathic PAH, and our preliminary results suggest that this would decrease endogenous PPARγ activity. Hence, a strategy

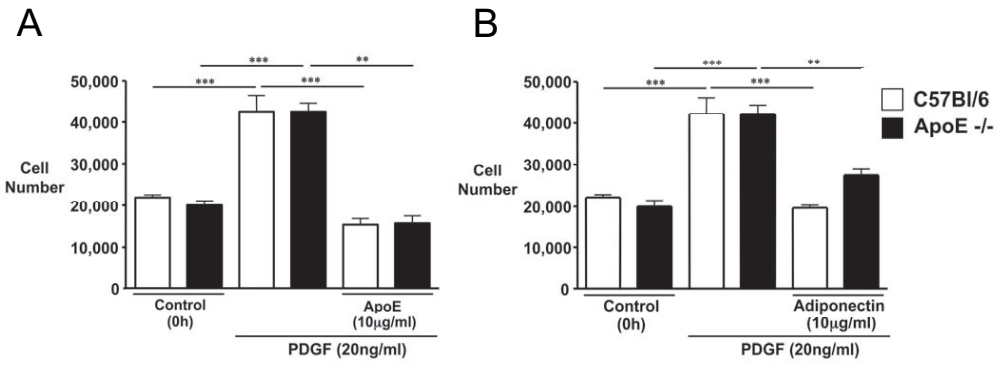

Figure 4. Recombinant apoE (A) and adiponectin (B) inhibit PDGF-BB–induced (20 ng/mL) proliferation of murine PASMC harvested both from C57Bl/6 and apoE$^{-/-}$ mice. Bars represent mean±SEM (n=3). *$P<0.05$; **$P<0.01$; and ***$P<0.001$.

aimed at activating PPARγ could reverse the PAH phenotype. However, the inheritance pattern of BMPR-II is that of a dominant gene with low penetrance in that only ≈20% of affected family members develop the disease.[51] This underscores the importance of environmental modifiers like insulin resistance that could potentiate BMP-RII dysfunction. It also is possible that abnormalities in downstream effectors of BMP-2 such as PPARγ and its targets may contribute to the development of disease.

The present study identified several new factors that may be involved in the pathogenesis of PAH and a potential treatment. We acknowledge that it is difficult to separate the effects of apoE deficiency and insulin resistance in our animal model and to extrapolate the potential impact of a successful experimental treatment to human disease. Therefore, it is important to examine whether insulin resistance, hyperlipidemia, impaired apoE function, and low adiponectin levels are risk factors for the progression of PAH in humans. It will also be of interest to investigate a relationship between molecular mechanisms that underlie insulin resistance, apoE and adiponectin levels, and known PAH pathways (eg, those downstream of BMP-RII). Taken together, these data might suggest a beneficial effect from the addition of PPARγ agonists to the treatment regimen for PAH patients.

Acknowledgments

We thank Tim Doyle for help with micro-CT imaging and Grant Hoyt for excellent technical assistance.

Sources of Funding

This work was supported by NIH (1-R01-HL074186–01) and the Dwight and Vera Dunlevie Endowed Professorship (Dr Rabinovitch), a postdoctoral fellowship from the American Heart Association/Pulmonary Hypertension Association (0425943H to Dr Hansmann), NIH grant HL876445–03 (Dr Wagner), and a predoctoral fellowship from Boehringer Ingelheim Funds (S. Schellong).

Disclosures

None.

References

1. Weiss R, Dziura J, Burgert TS, Tamborlane WV, Taksali SE, Yeckel CW, Allen K, Lopes M, Savoye M, Morrison J, Sherwin RS, Caprio S. Obesity and the metabolic syndrome in children and adolescents. *N Engl J Med*. 2004;350:2362–2374.
2. Eckel RH, Grundy SM, Zimmet PZ. The metabolic syndrome. *Lancet*. 2005;365:1415–1428.
3. Lazar MA. The humoral side of insulin resistance. *Nat Med*. 2006;12:43–44.
4. Ameshima S, Golpon H, Cool CD, Chan D, Vandivier RW, Gardai SJ, Wick M, Nemenoff RA, Geraci MW, Voelkel NF. Peroxisome proliferator-activated receptor gamma (PPARgamma) expression is decreased in pulmonary hypertension and affects endothelial cell growth. *Circ Res*. 2003;92:1162–1169.
5. He W, Barak Y, Hevener A, Olson P, Liao D, Le J, Nelson M, Ong E, Olefsky JM, Evans RM. Adipose-specific peroxisome proliferator-activated receptor gamma knockout causes insulin resistance in fat and liver but not in muscle. *Proc Natl Acad Sci U S A*. 2003;100:15712–15717.
6. Hevener AL, He W, Barak Y, Le J, Bandyopadhyay G, Olson P, Wilkes J, Evans RM, Olefsky J. Muscle-specific PPARg deletion causes insulin resistance. *Nat Med*. 2003;9:1491–1497.
7. Lehrke MM, Lazar MAMA. The many faces of PPARgamma. *Cell*. 2005;123:993–999.
8. Geraci MW, Moore M, Gesell T, Yeager ME, Alger L, Golpon H, Gao B, Loyd JE, Tuder RM, Voelkel NF. Gene expression patterns in the lungs of patients with primary pulmonary hypertension: a gene microarray analysis. *Circ Res*. 2001;88:555–562.
9. Greenow K, Pearce NJ, Ramji DP. The key role of apolipoprotein E in atherosclerosis. *J Mol Med*. 2005;83:329–342.
10. Combs CK, Johnson DE, Karlo JC, Cannady SB, Landreth GE. Inflammatory mechanisms in Alzheimer's disease: inhibition of beta-amyloid-stimulated proinflammatory responses and neurotoxicity by PPARgamma agonists. *J Neuroscience*. 2000;20:558–567.
11. Humbert M, Monti G, Brenot F, Sitbon O, Portier A, Grangeot-Keros L, Duroux P, Galanaud P, Simonneau G, Emilie D. Increased interleukin-1 and interleukin-6 serum concentrations in severe primary pulmonary hypertension. *Am J Respir Crit Care Med*. 1995;151:1628–1631.
12. Imaizumi T, Matsumiya T, Tamo W, Shibata T, Fujimoto K, Kumagai M, Yoshida H, Cui XF, Tanji K, Hatakeyama M, Wakabayashi K, Satoh K. 15-Deoxy-D12,14-prostaglandin J2 inhibits CX3CL1/fractalkine expression in human endothelial cells. *Immunol Cell Biol*. 2002;80:531–536.
13. Balabanian K, Foussat A, Dorfmuller P, Durand-Gasselin I, Capel F, Bouchet-Delbos L, Portier A, Marfaing-Koka A, Krzysiek R, Rimaniol AC, Simonneau G, Emilie D, Humbert M. CX(3)C chemokine fractalkine in pulmonary arterial hypertension. *Am J Respir Crit Care Med*. 2002;165:1419–1425.
14. Ikeda Y, Yonemitsu Y, Kataoka C, Kitamoto S, Yamaoka T, Nishida K, Takeshita A, Egashira K, Sueishi K. Anti-monocyte chemoattractant protein-1 gene therapy attenuates pulmonary hypertension in rats. *Am J Physiol Heart Circ Physiol*. 2002;283:H2021–H2028.
15. Martin-Nizard F, Furman C, Delerive P, Kandoussi A, Fruchart JC, Staels B, Duriez P. Peroxisome proliferator-activated receptor activators inhibit oxidized low-density lipoprotein-induced endothelin-1 secretion in endothelial cells. *J Cardiovasc Pharmacol*. 2002;40:822–831.
16. Giaid A, Yanagisawa M, Langleben D, Michel RP, Levy R, Shennib H, Kimura S, Masaki T, Duguid WP, Stewart DJ. Expression of endothelin-1 in the lungs of patients with pulmonary hypertension. *N Engl J Med*. 1993;328:1732–1739.
17. Yudkin JS, Eringa E, Stehouwer CD. "Vasocrine" signalling from perivascular fat: a mechanism linking insulin resistance to vascular disease. *Lancet*. 2005;365:1817–1820.
18. Stühlinger MC, Abbasi F, Chu JW, Lamendola C, McLaughlin TL, Cooke JP, Reaven GM, Tsao PS. Relationship between insulin resistance and an endogenous nitric oxide synthase inhibitor. *JAMA*. 2002;287:1420–1426.
19. Kielstein JT, Bode-Böger SM, Hesse G, Martens-Lobenhoffer J, Takacs A, Fliser D, Hoeper MM. Asymmetrical dimethylarginine in idiopathic pulmonary arterial hypertension. *Arterioscler Thromb Vasc Biol*. 2005;25:1414–1418.
20. Humbert M, Monti G, Fartoukh M, Magnan A, Brenot F, Rain B, Capron F, Galanaud P, Duroux P, Simonneau G, Emilie D. Platelet-derived growth factor expression in primary pulmonary hypertension: comparison of HIV seropositive and HIV seronegative patients. *Eur Respir J*. 1998;11:554–559.
21. Schermuly RT, Dony EE, Ghofrani HA, Pullamsetti S, Savai R, Roth M, Sydykov A, Lai YJ, Weissmann N, Seeger W, Grimminger F. Reversal of experimental pulmonary hypertension by PDGF inhibition. *J Clin Invest*. 2005;115:2811–2821.
22. Ghofrani HA, Seeger W, Grimminger F. Imatinib for the treatment of pulmonary arterial hypertension. *N Engl J Med*. 2005;353:1412–1413.
23. Ishigami M, Swertfeger DK, Granholm NA, Hui DY. Apolipoprotein E inhibits platelet-derived growth factor-induced vascular smooth muscle cell migration and proliferation by suppressing signal transduction and preventing cell entry to G1 phase. *J Biol Chem*. 1998;273:20156–20161.
24. Campbell M, Allen WE, Silversides JA, Trimble ER. Glucose-induced phosphatidylinositol 3-kinase and mitogen-activated protein kinase-dependent upregulation of the platelet-derived growth factor-beta receptor potentiates vascular smooth muscle cell chemotaxis. *Diabetes*. 2003;52:519–526.
25. Vantler M, Caglayan E, Zimmermann WH, Baumer AT, Rosenkranz S. Systematic evaluation of anti-apoptotic growth factor signaling in vascular smooth muscle cells: only phosphatidylinositol 3′-kinase is important. *J Biol Chem*. 2005;280:14168–14176.
26. Yamauchi T, Kamon J, Waki H, Terauchi Y, Kubota N, Hara K, Mori Y, Ide T, Murakami K, Tsuboyama-Kasaoka N, Ezaki O, Akanuma Y, Gavrilova O, Vinson C, Reitman ML, Kagechika H, Shudo K, Yoda M, Nakano Y, Tobe K, Nagai R, Kimura S, Tomita M, Froguel P, Kadowaki T. The fat-derived hormone adiponectin reverses insulin resistance associated with both lipoatrophy and obesity. *Nat Med*. 2001;7:941–946.

27. Arita Y, Kihara S, Ouchi N, Maeda K, Kuriyama H, Okamoto Y, Kumada M, Hotta K, Nishida M, Takahashi M, Nakamura T, Shimomura I, Muraguchi M, Ohmoto Y, Funahashi T, Matsuzawa Y. Adipocyte-derived plasma protein adiponectin acts as a platelet-derived growth factor-BB-binding protein and regulates growth factor-induced common postreceptor signal in vascular smooth muscle cell. *Circulation.* 2002;105:2893–2898.
28. Boucher P, Gotthardt M, Li WP, Anderson RG, Herz J. LRP: role in vascular wall integrity and protection from atherosclerosis. *Science*. 2003; 300:329–332.
29. Boucher P, Gotthardt M. LRP and PDGF signaling: a pathway to atherosclerosis. *Trends Cardiovasc Med*. 2004;14:55–60.
30. Newton CS, Loukinova E, Mikhailenko I, Ranganathan S, Gao Y, Haudenschild C, Strickland DK. Platelet-derived growth factor receptor-beta (PDGFR-beta) activation promotes its association with the low density lipoprotein receptor-related protein (LRP): evidence for co-receptor function. *J Biol Chem.* 2005;280: 27872–27878.
31. Wang Y, Lam KS, Xu JY, Lu G, Xu LY, Cooper GJ, Xu A. Adiponectin inhibits cell proliferation by interacting with several growth factors in an oligomerization-dependent manner. *J Biol Chem.* 2005;280:18341–18347.
32. Lassila M, Allen TJ, Cao Z, Thallas V, Jandeleit-Dahm KA, Candido R, Cooper ME. Imatinib attenuates diabetes-associated atherosclerosis. *Arterioscler Thromb Vasc Biol*. 2004;24:935–942.
33. Marx NN, Duez HH, Fruchart JCJ-C, Staels BB. Peroxisome proliferator-activated receptors and atherogenesis: regulators of gene expression in vascular cells. *Circ Res*. 2004;94:1168–1178.
34. Law RRE, Goetze SS, Xi XXP, Jackson SS, Kawano YY, Demer LL, Fishbein MMC, Meehan WWP, Hsueh WWA. Expression and function of PPARgamma in rat and human vascular smooth muscle cells. *Circulation*. 2000;101:1311–1318.
35. Xu A, Chan KW, Hoo RL, Wang Y, Tan KC, Zhang J, Chen B, Lam M, Tse C, Cooper GJ, Lam KS. Testosterone selectively reduces the high molecular weight form of adiponectin by inhibiting its secretion from adipocytes. *J Biol Chem*. 2005;280:18073–18080.
36. Fouty BW, Grimison B, Fagan KA, Le Cras TD, Harral JW, Hoedt-Miller M, Sclafani RA, Rodman DM. p27(Kip1) is important in modulating pulmonary artery smooth muscle cell proliferation. *Am J Respir Cell Mol Biol*. 2001;25:652–658.
37. St John Sutton M, Rendell M, Dandona P, Dole JF, Murphy K, Patwardhan R, Patel J, Freed M. A comparison of the effects of rosiglitazone and glyburide on cardiovascular function and glycemic control in patients with type 2 diabetes. *Diabetes Care*. 2002;25:2058–2064.
38. Wagenvoort CA. Pulmonary atherosclerosis. In: Wagenvoort CA, Heath D, Edwards JE, eds. *The Pathology of the Pulmonary Vasculature*. Springfield, Ill: Charles C Thomas; 1964:58–59.
39. Guignabert C, Izikki M, Tu LI, Li Z, Zadigue P, Barlier-Mur AM, Hanoun N, Rodman D, Hamon M, Adnot S, Eddahibi S. Transgenic mice overexpressing the 5-hydroxytryptamine transporter gene in smooth muscle develop pulmonary hypertension. *Circ Res*. 2006;98:1323–1330.
40. Merklinger SL, Jones PL, Martinez EC, Rabinovitch M. Epidermal growth factor receptor blockade mediates smooth muscle cell apoptosis and improves survival in rats with pulmonary hypertension. *Circulation*. 2005;112:423–431.
41. Long L, MacLean MR, Jeffery TK, Morecroft I, Yang X, Rudarakanchana N, Southwood M, James V, Trembath RC, Morrell NW. Serotonin increases susceptibility to pulmonary hypertension in BMPR2-deficient mice. *Circ Res*. 2006;98:818–827.
42. West J, Fagan K, Steudel W, Fouty B, Lane K, Harral J, Hoedt-Miller M, Tada Y, Ozimek J, Tuder R, Rodman DM. Pulmonary hypertension in transgenic mice expressing a dominant-negative BMPRII gene in smooth muscle. *Circ Res*. 2004;94:1109–1114.
43. Spranger J, Kroke A, Möhlig M, Bergmann MM, Ristow M, Boeing H, Pfeiffer AF. Adiponectin and protection against type 2 diabetes mellitus. *Lancet*. 2003;361:226–228.
44. Phillips JW, Barringhaus KG, Sanders JM, Yang Z, Chen M, Hesselbacher SS, Czarnik AC, Ley K, Nadler J, Sarembock IJ. Rosiglitazone reduces the accelerated neointima formation after arterial injury in a mouse injury model of type 2 diabetes. *Circulation*. 2003;108:1994–1999.
45. Zhang J, Fu M, Zhao L, Chen YE. 15-Deoxy-prostaglandin J(2) inhibits PDGF-A and -B chain expression in human vascular endothelial cells independent of PPAR gamma. *Biochem Biophys Res Commun*. 2002;298:128–132.
46. Goetze S, Kintscher U, Kim S, Meehan WP, Kaneshiro K, Collins AR, Fleck E, Hsueh WA, Law RE. Peroxisome proliferator-activated receptor-gamma ligands inhibit nuclear but not cytosolic extracellular signal-regulated kinase/mitogen-activated protein kinase-regulated steps in vascular smooth muscle cell migration. *J Cardiovasc Pharmacol*. 2001;38:909–921.
47. Wakino S, Kintscher U, Liu Z, Kim S, Yin F, Ohba M, Kuroki T, Schonthal AH, Hsueh WA, Law RE. Peroxisome proliferator-activated receptor gamma ligands inhibit mitogenic induction of p21(Cip1) by modulating the protein kinase Cdelta pathway in vascular smooth muscle cells. *J Biol Chem*. 2001;276:47650–47657.
48. Gauthier A, Vassiliou G, Benoist F, McPherson R. Adipocyte low density lipoprotein receptor-related protein gene expression and function is regulated by peroxisome proliferator-activated receptor gamma. *J Biol Chem*. 2003;278:11945–11953.
49. Bruemmer D, Yin F, Liu J, Berger JP, Sakai T, Blaschke F, Fleck E, Van Herle AJ, Forman BM, Law RE. Regulation of the growth arrest and DNA damage-inducible gene 45 (GADD45) by peroxisome proliferator-activated receptor gamma in vascular smooth muscle cells. *Circ Res*. 2003;93:e38–e47.
50. Hansmann G, Rabinovitch M. Bone morphogenetic protein 2 (BMP-2) activates the transcription factor, peroxisome proliferator-activated receptor gamma (PPARγ), in human pulmonary artery smooth muscle cells (HPASMC). *Circulation*. 2005;112:II-154. Abstract.
51. Lane KB, Machado RD, Pauciulo MW, Thomson JR, Phillips JA 3rd, Loyd JE, Nichols WC, Trembath RC. Heterozygous germline mutations in BMPR2, encoding a TGF-beta receptor, cause familial primary pulmonary hypertension: the International PPH Consortium. *Nat Genet*. 2000;26:81–84.

CLINICAL PERSPECTIVE

Recent studies document an increased incidence of metabolic syndrome and associated insulin resistance in children, adolescents, and adults, placing them at risk for systemic cardiovascular disease. Insulin resistance also may be linked to pulmonary arterial hypertension (PAH) because reduced expression of apolipoprotein E (apoE) and peroxisome proliferator–activated receptor-γ (PPARγ), which is associated with insulin resistance, is observed in lung tissues from PAH patients. Decreased levels of apoE and the PPARγ target adiponectin may enhance platelet-derived growth factor-BB signaling in pulmonary artery smooth muscle cells in a manner similar to that observed in systemic smooth muscle cells. In keeping with these observations, we now report a novel animal model in which PAH is linked to insulin resistance and reversed by PPARγ activation. Male apoE-deficient ($apoE^{-/-}$) mice on a high-fat diet do not upregulate the insulin sensitizers adiponectin and leptin (in contrast to control mice) but instead develop insulin resistance and severe PAH. Female $apoE^{-/-}$ mice on high-fat diet have higher adiponectin levels and less severe PAH than male $apoE^{-/-}$ mice. A 4-week treatment with the PPARγ agonist rosiglitazone led to an 8-fold increase in plasma adiponectin, improved insulin sensitivity, and complete regression of PAH in male insulin-resistant $apoE^{-/-}$ mice. We also document that apoE and adiponectin inhibit platelet-derived growth factor-BB–induced proliferation of pulmonary artery smooth muscle cells in culture. Our data suggest that insulin resistance, low plasma adiponectin levels, and apoE deficiency may be risk factors for PAH that can be reversed by PPARγ activation. Hence, PPARγ agonists could be given consideration in the treatment of PAH patients, particularly those with documented insulin resistance.

Supplementary Methods

Experimental Design. At 4 weeks of age, the mice were either continued on regular chow or switched to non-cholate-containing high fat diet, which included 21% anhydrous milk fat and 0.15% cholesterol (Dyets #101511, Dyets Inc.) for a maximal period of 21 weeks. *For the non-treatment study*, 15-week-old male and female mice (ApoE -/-, C57Bl/6 controls) on either diet were studied in room air (FiO_2 0.21). *For the rosiglitazone treatment study,* the drug dose per kg high fat diet was based on our own measurements of food intake (3g daily food intake per mouse) and a previous publication[1]. During the course of the study, the drug dose was adjusted once to weight gain in both mouse strains. All studies were carried out under a protocol approved by the Stanford Animal Care Committee following the guidelines of the American Physiological Society.

Hemodynamic Measurements. *RV and LV catheterization:* Measurements of RVSP and RV dp/dt were performed under isoflurane anesthesia (1.5-2.5%) using a closed chest technique in unventilated mice at 15, 19 and 25 weeks of age. Briefly, a 1.4 F catheter (Millar Instruments, Houston, Texas) was inserted into the right jugular vein and then placed into the free RV cavity. Using the PowerLab/4SP recording unit (AD Instruments, Colorado Springs, CO), 3-5 simultaneous tracings from different time points were taken to determine the individual RVSP, maximal rate of pressure development (RV dp/dt max.; RV systolic function) and maximal rate of pressure decay (RV dp/dt min.; RV diastolic function). Left ventricular enddiastolic pressure (LVEDP) was determined by direct LV catheterization under isoflurane anesthesia (2.5%). Briefly, a 1.4F catheter tip (Millar Instruments, Houston, TX) was inserted through the left carotid artery and advanced in a retrograde fashion past the aortic valve, into the left ventricular cavity. The catheter was adjusted to lie in the left ventricular outflow tract and tracings were evaluated in real time to ensure adequate catheter placement. Data were recorded using the PowerLab

system (ADInstruments, Colorado Springs, CO). LVEDP was determined using PVAN 3.4 software (Millar Instruments, Houston, TX). *Systemic blood pressure* was determined in non-anesthetized mice by the tail cuff method using the BP 2000 analysis system (Visitech Systems, Apex, NC). At least 5 recordings per mouse were taken to determine systolic BP, MAP and diastolic BP. *Echocardiography:* Measurements of cardiac output and function were performed by echocardiography in mice anesthetized with ketamine (70 mg/kg i.p.) and xylazine (12 mg/kg i.p.) using an ultrasound machine (Vivid 7, GE Medical Systems) equipped with a 13 MHZ linear array transducer. Fractional shortening (FS) and heart rate (HR) were determined in M-mode. Ejection fraction (EF) and cardiac output (CO) were estimated using the Teichholz formula[2]. In addition to the invasively measured RV dp/dt., the Tei-Index ([isovolumetric contraction time + isovolumetric relaxation time]/ ejection time) was calculated in a subset of animals to reveal any potential RV dysfunction[3, 4].

Right and Left Ventricular Hypertrophy. Right ventricular hypertrophy (RVH) was measured as described[5] by the weight of the right ventricle relative to left ventricle (LV) + septum. Left ventricular hypertrophy (LVH) was measured as absolute weight of the LV plus septum, and as enddiastolic interventricular septum thickness (IVSd) by echocardiographic M-mode imaging. LV dilatation was assessed by echocardiographic M-mode measurement of the LV enddiastolic inner diameter.

Lung tissue preparation. After abdominal aortic dissection, lungs were perfused *in vivo* by injecting 5ml normal saline into the beating RV. Lungs were tracheally injected with 10% formalin, fixed overnight, and then embedded either in paraffin for standard histology (Hematoxylin & Eosin, Elastic van Gieson, Movat pentachrome) or treated with sucrose-gradient solution (15-30%) and frozen in OCT (Tissue Tek) for Oil-red-O (fat) staining[6]. Prior to fixation, a subset of left lungs (approximately half) were barium-infused via PA-inserted tubing[7] to label

peripheral pulmonary arteries for morphometric analysis and micro-CT-imaging. The barium was infused by hand with similar gross and microscopic endpoints of pre-capillary filling of all small vessels at alveolar duct and wall level.

Morphometric Analysis. Transverse left lung sections (3 step sections, 200μm apart) were stained by Elastic van Gieson and Movat pentachrome. Muscularized and non-muscularized peripheral (alveolar wall) pulmonary arteries were counted in 5-10 random views per lung.

Micro-CT-Imaging. A custom-built eXplore Locus RS120 Micro CT Scanner (GE Health Care, Ontario, Canada) was used to acquire non-destructing 3-D images of barium-infused [7] whole lung specimens.

Oil-red-O (fat) Staining. Oild-red-O (fat) staining of fresh frozen lung sections was performed as previously described [6].

Cell Culture and Functional Assays: *Primary murine PASMC were isolated from* 5 male 14-15-week old mice of either genotype on regular chow and used for one culture: The main extralobular pulmonary arteries were dissected, cleaned from adherent tissue, cut in small pieces and digested for 90 min. in dispersion media containing 0.53mg/ml elastase (Roche), 0.53mg/ml collagenase II (Worthington), 2mg/ml albumin (Sigma), 0.2mg/ml soybean trypsin inhibitor (Worthington), 40 μM $CaCl_2$, in HBSS buffer (Gibco). PASMC were then cultured in DMEM (Gibco) containing FBS (20% for 3 days, then reduced to 10%), 2mM L-glutamine and 100U/ml Penicillin, 0.1mg/ml streptomycin. Passages 3-4 were used for further studies. Smooth muscle cell identity was verified by positive immunohistochemistry staining for SM α-actin (Sigma) (> 95% of cells stained positive for SM α-actin). PASMC were grown to 70% confluence and then cultured for 24h in starvation media (DMEM, 0.1% FBS, 2mM L-glutamine, 100U/ml Penicillin, 0.1mg/ml streptomycin). The media with or without growth factors and/or inhibitors was changed every 24h.

Cell Counts: PASMC were seeded at $2.5x10^4$ cells per well of a 24-well plate in 500µl of growth medium and allowed to adhere overnight. The medium was removed and the cells washed 3 times with PBS prior to the addition of starvation media (DMEM, 0.1% FBS, penicillin/streptomycin) and incubated at 37°C, 5% CO_2 for 24 (murine PA SMC) or 48h (human PA SMC) prior to PDGF-BB stimulation for 0h and 72h (treatments and concentrations stated in the figure legends). Cells were washed twice with PBS and trypsinized in 150µl of Trypsin/EDTA (Cascade Biologics) for 7min., followed by the addition of 150µl trypsin neutralizer (Cascade Biologics). The cells were then resuspended and counted in a hemacytometer (4 counts per well and condition).

Whole blood and blood plasma measurements. Since even brief isoflurane exposure elevates plasma glucose levels in mice *in vivo* [8], we performed tail vein puncture in non-anesthetized, overnight-starved mice followed by immediate, duplicate whole blood glucose measurements with a glucometer (Freestyle/Abbott). Fasting blood plasma was obtained either via retroorbital bleeding or – in a subset of mice – by cardiac puncture, either after cervical dislocation or under isoflurane anesthesia. Fasting plasma adiponectin and insulin levels were determined by radioimmunosorbent assay (RIA), plasma leptin values as duplicate measurements by a multiplex cytokine assay at Linco Diagnostics (St. Charles, MO). Plasma endothelin-1 was assessed by enzyme-linked immunosorbent assay (ELISA). Total cholesterol (Roche Diagnostics), HDL-cholesterol (L-type HDL-cholesterol assay, Wako Diagnostics) and triglycerides (triglycerides glycerol blanked assay, Roche Diagnostics) were measured with commercially available enzymatic kits on a Hitachi 917 analyzer.

References (Online Data Supplement)

1. Ueshima K, Akihisa-Umeno H, Nagayoshi A, Takakura S, Matsuo M, Mutoh S. A gastrointestinal lipase inhibitor reduces progression of atherosclerosis in mice fed a western-type diet. *Eur J Pharmacol.* 2004;501:137-142.
2. Teichholz LE, Kreulen T, Herman MV, Gorlin R. Problems in echocardiographic volume determinations: echocardiographic-angiographic correlations in the presence of absence of asynergy. *Am J Cardiol.* 1976;37:7-11.
3. Tei C, Ling LH, Hodge DO, Bailey KR, Oh JK, Rodeheffer RJ, Tajik AJ, Seward JB. New index of combined systolic and diastolic myocardial performance: a simple and reproducible measure of cardiac function--a study in normals and dilated cardiomyopathy. *J Cardiol.* 1995;26:357-366.
4. Grignola JC, Gines F, Guzzo D. Comparison of the Tei index with invasive measurements of right ventricular function. *Int J Cardiol.* 2005.
5. Zaidi SH, You XM, Ciura S, Husain M, Rabinovitch M. Overexpression of the serine elastase inhibitor elafin protects transgenic mice from hypoxic pulmonary hypertension. *Circulation.* 2002;105:516-521.
6. Johnson FB. Lipids. In: Prophet EB, Mills B, Arrington J, et al., eds. *Laboratory Methods in Histotechnology.* 2nd ed. Washington, D.C.: American Registry of Pathology; 1994:175-182.
7. Ye CL, Rabinovitch M. Inhibition of elastolysis by SC-37698 reduces development and progression of monocrotaline pulmonary hypertension. *Am J Physiol.* 1991;261:H1255-1267.
8. Pomplun D, Mohlig M, Spranger J, Pfeiffer AF, Ristow M. Elevation of blood glucose following anaesthetic treatment in C57BL/6 mice. *Horm Metab Res.* 2004;36:67-69.

Supplement Table 1. Metabolic measurements in *male* C57Bl/6 (control) and apoE -/- mice in normoxia

	Regular Chow (Normoxia)		High Fat Diet (Normoxia)			
Parameter	**Control (CR)**	**ApoE -/- (AR)**	**Control (CF)**	**ApoE -/- (AF)**	**P-value**	**N**
Blood Glucose (mg/dl)	94 ± 5.4	76 ± 2.5	85 ± 7.5	148 ± 7.4***	***AF vs CF; ***AF vs AR	5-10
Plasma Insulin (ng/ml)	0.64 ± 0.12	0.35 ± 0.15	0.50 ± 0.24	1.19 ± 0.21*	*AF vs AR	4-10
Plasma Adiponectin (µg/ml)	4.6 ± 0.57	6.2 ± 0.87	8.5 ± 0.45**	7.1 ± 0.60	**CF vs CR	4-6
Plasma Leptin (mg/dl)	318 ± 101	437 ± 96	15015 ± 4536**	2642 ± 784*	**CF vs CR; *AF vs CF	3-6
Total Cholesterol (mg/dl)	100 ± 4.3	457 ± 32.7***	166 ± 18.6	1198 ± 23.1***	***AR vs CR; ***AF vs AR; ***AF vs CF	4-6
HDL-Cholesterol (mg/dl)	74 ± 3.3	66 ± 9.3	132 ± 15.2**	108 ± 7.2	**CF vs CR	4-6
Non-HDL-Cholesterol (mg/dl)	26 ± 2.7	391 ± 33.0***	34 ± 3.5	1099 ± 20.1***	***AR vs CR; ***AF vs AR; ***AF vs CF	4-6
Triglycerides (mg/dl)	59 ± 5.5	128 ± 17.0**	72 ± 8.8	121 ± 7.4	**AR vs CR	4-6

Supplement Table 1. 15 week-old male mice, on regular chow or high fat diet for 11 weeks, in normoxia. Statistically significant differences between C57Bl/6 (control) and apoE -/- mice on either regular chow or high fat diet, and differences between mice of the same genotype on either diet are indicated. * $p<0.05$; ** $p<0.01$; *** $p<0.001$.

Supplement Table 2. Metabolic measurements in *female* C57Bl/6 (control) and apoE -/- mice in normoxia

	Regular Chow (Normoxia)		High Fat Diet (Normoxia)			
Parameter	**Control (CR)**	**ApoE -/- (AR)**	**Control (CF)**	**ApoE -/- (AF)**	**P-value**	**n**
Blood Glucose (mg/dl)	85 ± 4.1	79 ± 6.9	105 ± 8.9**	77 ± 3.0	** CF vs AF	5-10
Plasma Insulin (ng/ml)	0.26 ± 0.08	0.09 ± 0.04	0.46 ± .10	0.29 ± 0.05		4-11
Plasma Adiponectin (µg/ml)	8.9 ± 0.8	12.5 ± 1.1	19.1 ± 2.5***	11.2 ± 0.43***	***CF vs CR; **AF vs CF	4-9
Plasma Leptin (mg/dl)	2279 ± 540	649 ± 112	13560 ± 6980*	821 ± 184*	*CF vs CR; ; *AF vs CF	4-9
Total Cholesterol (mg/dl)	59 ± 4.8	408 ± 15.4***	129 ± 14.1	1159 ± 27.6***	***AR vs CR; ***AF vs AR; ***AF vs CF	4-7
HDL-Cholesterol (mg/dl)	40 ± 8.0	44 ± 6.1	94 ± 16.1*	70 ± 12.2	*CF vs CR	4-7
Non-HDL-Cholesterol (mg/dl)	19 ± 4.3	364 ± 12.0***	35 ± 4.4	1089 ± 28.9***	***AR vs CR; ***AF vs AR; ***AF vs CF	4-7
Triglycerides (mg/dl)	82 ± 5.5	97 ± 9.3	54 ± 5.6	120 ± 7.0***	***AF vs CF	4-7

Supplement Table 2. 15 week-old female mice, on regular chow or high fat diet for 11 weeks, in normoxia. Statistically significant differences between C57Bl/6 (control) and apoE -/- mice on either regular chow or high fat diet, and differences between mice of the same genotype on either diet are indicated. * $p<0.05$; ** $p<0.01$; *** $p<0.001$.

Supplement Table 3. Metabolic, hemodynamic, echocardiographic, heart weight and hematocrit measurements in *male* C57Bl/6 (control) and apoE -/- mice after 10-week treatment with rosiglitazone

Parameter	Control (C)	Control Rosi (CR)	ApoE -/- (A)	ApoE-/- Rosi (AR)	P-Value	N
Body weight (g)	35.1 ± 3.6	31.2 ± 2.0	47.5 ± 1.4**	48.5 ± 2.4***	**A vs C; ***AR vs CR	8-9
Metabolism						
Blood Glucose (mg/dl)	90 ± 7.4	77 ± 5.3	137 ± 5.7***	98 ± 5.6***	***A vs C; ***AR vs A	8-9
HgA1c (%)	3.81 ± 0.10	3.52 ± 0.13	4.18 ± 0.13	3.85 ± 0.12		5-8
Hemodynamics						
RVSP (mmHg)	22.3 ± 0.2	22.2 ± 0.7	28.3 ± 0.5***	24.4 ± 0.5***	***A vs C; ***AR vs A	5-8
RV dp/dt max (mmHg/s)	1477 ± 76.5	1408 ± 104.7	1601 ± 46.6	1580 ± 94.9		5-8
RV dp/dt min (mmHg/s)	-1262 ± 75.6	-1134 ± 60.0	-1521 ± 64.2	-1383 ± 106.0		5-8
Systolic BP (mmHg) †	103 ± 3.4	95 ± 2.4	108 ± 4.0	100 ± 2.3		7-8
MAP (mmHg) †	85 ± 3.3	78 ± 2.6	90 ± 4.2	81 ± 3.3		7-8
Diastolic BP (mmHg) †	75 ± 3.3	70 ± 2.8	81 ± 4.4	71 ± 3.9		7-8
Echocardiography						
Heart Rate (bpm)	313 ± 11.7	351 ± 15.6	360 ± 11.5	341 ± 11.4		6-8
EF (%)	68.2 ± 1.9	65.1 ± 1.1	68.9 ± 1.0	62.9 ± 0.8*	*AR vs A	6-8
FS (%)	33.0 ± 1.3	30.8 ± 0.8	33.4 ± 0.8	29.3 ± 0.5*	*AR vs A	6-8
CO (ml/min)	38.5 ± 2.3	44.3 ± 2.6	44.4 ± 2.3	50.0 ± 3.4		6-8
LVIDD (mm)	4.20 ± 0.10	4.26 ± 0.06	4.23 ± 0.10	4.58 ± 0.16		6-8
LVISD (mm)	2.81 ± 0.11	2.95 ± 0.05	2.83 ± 0.06	3.23 ± 0.13*	*AR vs A	6-8
LVPWd (mm)	0.69 ± 0.05	0.79 ± 0.07	0.64 ± 0.04	0.60 ± 0.06		6-8
IVSd (mm)	0.89 ± 0.10	0.96 ± 0.07	0.84 ± 0.07	0.87 ± 0.10		6-8
TEI-Index	0.51 ± 0.06	0.60 ± 0.04	0.77 ± 0.14	0.61 ± 0.04		6-8
Heart weight						
RV (mg)	23.5 ± 1.5	26.8 ± 1.5	35.5 ± 1.4***	29.3 ± 1.9	***A vs C	6
RV/LV+S	0.24 ± 0.01	0.25 ± 0.02	0.43 ± 0.02***	0.25 ± 0.02***	***A vs C; ***AR vs A	6
LV+S (mg)	96.2 ± 3.7	110.0 ± 5.7	82.3 ± 3.2	117.0 ± 7.5**	**AR vs A	6
Blood						
HCT (%)	46.3 ± 2.0	40.6 ± 0.9*	48.8 ± 0.5	42.2 ± 1.2*	*CR vs C; *AR vs A	6-8
WBC (x10^3 cells/µL)	5.6 ± 1.1	10.1 ± 2.3	8.0 ± 1.5	6.7 ± 1.2		6-7

Supplement Table 3. 25 week-old male mice on high fat diet for 21 weeks, untreated or treated with rosiglitazone (Rosi) for 10 weeks, in normoxia. Statistically significant differences between C57Bl/6 (control) and apoE -/- mice of either group, and between treated and untreated mice of the same genotype are indicated. ∗ $p<0.05$; ∗∗ $p<0.01$; ∗∗∗ $p<0.001$. HgA1c, glucosylated hemoglobin A1c; RVSP, right ventricular systolic pressure; dp/dt max., maximal rate of pressure development (systolic RV function); dp/dt min., max. rate of pressure decay (diastolic RV function); BP, blood pressure; MAP, mean arterial pressure; EF, ejection fraction; FS, fractional shortening; CO, cardiac output; LVIDD, left-ventricular enddiastolic inner diameter; LVISD, left-ventricular endsystolic inner diameter; LVPWd, left-ventricular enddiastolic posterior wall thickness; IVSd, end-diastolic interventricular septum thickness; Tei-Index, parameter of RV dysfunction ([isovolumetric contraction time + isovolumetric relaxation time]/ ejection time); ; RV, right ventricle; LV+S, left ventricle plus septum; HCT, hematocrit; WBC, white blood cell count. † Systemic blood pressure was measured at 24 weeks of age, i.e. after treatment with rosiglitazone for 9 weeks.

Supplement Figure 1:

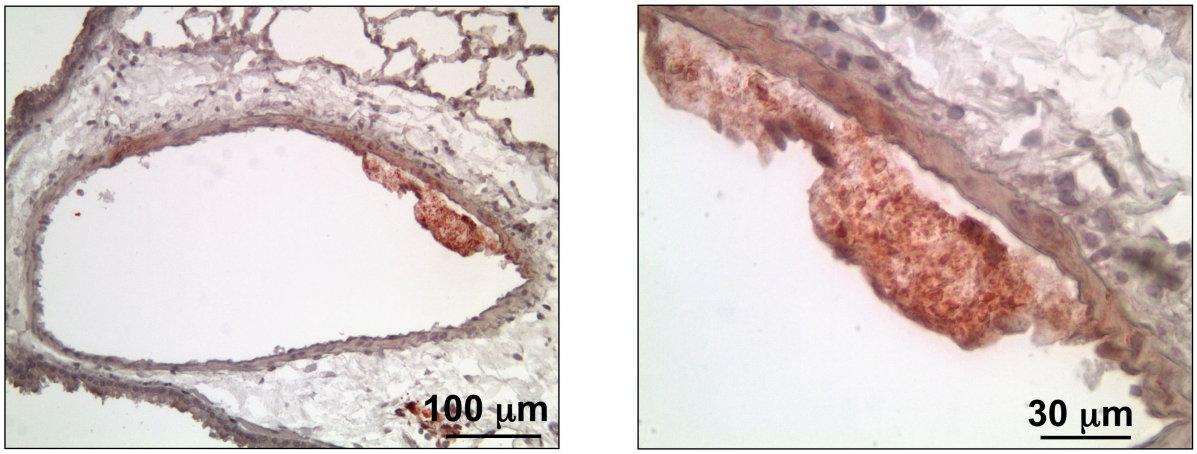

Supplementary Figure 1. Non-occlusive, atherosclerotic lesion in a large intrapulmonary artery of an apoE -/- mouse on high fat diet.

Representative Oil-red-O (fat) photomicrographs of a histological section taken from the lung of a 15-week old apoE-/- mouse on high fat diet for 11 weeks. Atherosclerotic plaques were neither observed in smaller pulmonary arteries (less than 500μm) of apoE -/- mice on high fat diet, nor in apoE -/- on regular chow or in C57/Bl6 mice on either diet.